EUROPEAN JOURNAL OF LIFE SAFETY AND STABILITY (EJLSS)
ISSN2660-9630
www.ejlss.indexedresearch.org Volume 30, Jun-2023 ||

An Investigation into the Effects of Waste Glass Powder on the Condition of the Soil

Alwina Khatun Ansari, Prathiba. P, Preetha. S
Bachelor of Engineering, Department of Civil Engineering, Dhaanish Ahmed College of Engineering, Chennai, Tamil Nadu, India

M. Nisha, M. Saranya
Assistant Professor, Department of Civil Engineering, Dhaanish Ahmed College of Engineering, Chennai, Tamil Nadu, India

Abstract: *Soil stabilisation enhances the engineering properties of soils by alteration of the physical properties of the soil. It also increases the shear strength of soil, controls its shrink-swell properties and improves the load-bearing capacity of soils. Sustainable soil stabilisation relies heavily on recycling materials like old glass, plastic, and rubber. In particular, weak soils necessitate the use of effective soil stabilisation procedures to maintain sufficient stability. Soil stabilisation is one potential benefit of industrial wastes that are neither biodegradable nor compostable. Here, the soil has been stabilised with discarded glass powder, which is not biodegradable. Glass, being an inert material, cannot be broken down by natural processes. Similarly, to how natural rock deteriorates, it loses its integrity over time. Because of its inert nature, it can be used to fortify a wide range of soil and road-building components. Several experiments, including Specific Gravity, Atterberg limits, Standard Proctor Test, California Bearing Test, and Unconfined Compression Test, were conducted with varying percentages of glass powder and the results are described.*

Keywords: *Waste Glass Powder, Condition of the Soil, Asan inert construction, Freeze/thaw cycles, Specific Gravity.*

Date of Submission: 06-05-2023 ***Date of Acceptance: 28-06-2023***

Introduction

When soil is stabilised, its physical qualities are altered to increase its strength irreversibly before construction begins. When planning, designing, and building with stabilised soils in mind, the results are superior to those with unstabilised soils [14]. By incorporating the stabilised soil layer into the pavement's structural design, future layers can be thinner, reducing the requirement for virgin materials and saving significantly on costs. As a solid monolith, stabilised soil minimises permeability, lessening the potential for shrinkage/expansion and the damaging impacts of freeze/thaw cycles. Removal and replacement of soil may not always be necessary if it can be stabilised in place or by natural means [15]. Frequently, construction locations for pavement constructions like highways, building pads, parking lots, runways, etc., have naturally moist, weak soils. Stabilization adds strength, and technical qualities like moisture content and flexibility can be improved through chemical treatment. Although methods of soil stabilisation that occur away from the actual construction site are technically feasible, they are often only used for environmental

projects [16]. Lighter loads are more likely to experience difficulties in clay soil than moderate ones. These issues appear as clay, shrinkage, and unequal settlement because the soil consolidates under load and changes volumetrically long with seasonal moisture variation [17]. Soil stabilisation techniques have been used to enhance soil qualities for thousands of years. Strength enhancement and plasticity behaviour studies have been conducted using a variety of locally available stabilising chemicals, such as waste plastic powder. Waste glass powder and clayey soil were mixed in varying quantities to create the admixtures [18].

Objectives

- Because the soils are so weak, they need to be stabilised.
- So that the building doesn't sink as much into the ground.
- In order to boost the soil's bearing capacity by increasing its shear strength
- Lessen the soil's tendency to contract and expand.
- Reduce embankment and dam slope collapse risk caused by soil strength variation.
- For one to consider waste management from a new perspective.

Existing Methods to Stabilise Soils

Cement Stabilisation

Because of its low cost and versatility, cement has been a go-to soil stabiliser for many projects [19]. It has cutting-edge characteristics, so they say. Cement is one of the cheapest binders in many regions of the world, but its unit price varies substantially based on the distribution network and the closeness of the cement manufacturing plant. The first step in applying cement for soil stabilisation is to calculate how much cement and water will be required for the job. Careful management of the soil-cement mixture's moisture content is required [20]. The cement won't hydrate properly without enough water. The ultimate density, porosity, water/cement ratio, final strength, and shrinkage cracking can all be negatively impacted by adding too much water [21]. The amount of cement to be added is typically established through laboratory testing, unless qualities are known from past projects using the same pavement components. In most cases, simple field-based tests are used to regulate water levels in the field during the time of construction. Specialized cement spreaders or hopper trucks often transport and distribute the cement across the finely ground soil. Typically, a moisture level of 1%-2% below the optimum compaction requirement is sought. Before the mixture sets, the reaction can be carried out. Depending on the cement's properties, the waiting period between adding water and compacting might be anywhere from one to four hours [22-25].

Sheepsfoot is used first, followed by steel drum and pneumatic-tired rollers, to compact the mixture. A grader and steel drum roller are required to refine the impressions left by the sheep foot. Used to impart a tight surface texture, rollers with pneumatic tyres [26]. When cement is mixed with water, a gel forms around the cement particles and expands to form a matrix that coats the soil particles and holds them together. Cement's impact on soil stabilisation may be due to the formation of an agglomerated structure of calcium silicate hydrates and calcium hydroxide, which binds neighbouring particles, or to a reduction in the material's flexibility and increased resistance to moisture. The latter can improve tensile strength, which can then crack under stress or because of cement shrinkage as it dries. As a result, many people who own roads view shrinkage cracking as a negative outcome [27]. Let's pretend that the stabilised material contains a size distribution with a considerable fraction of particles smaller than 425 microns. These small particles inhibit the cementitious process, making cement application in soil stabilisation less than ideal [28-30].

Drawbacks of Soil Cement Stabilisation:

It doesn't work well with every soil type; high dosages might cause brittle failure mechanisms, ugly shrinkage cracking that lets water in, and more damage from large or heavy vehicles than more flexible materials. [31]

Lime Stabilization

Quicklime (calcium oxide), hydrated lime (calcium hydroxide), and lime slurry are all effective forms of lime for use in soil stabilisation. Calcium carbonate (limestone) is converted into quicklime via chemical oxidation. Quicklime and water combine to form hydrated lime, and lime slurry is a hydrated lime suspension in water. At least 25% of the soil must pass the #200 sieve (74mm) for the soil to be regarded eligible for lime treatment, and the soil's Plasticity Index must be more than ten. Soil stabilisation using lime is not recommended for areas where the percentage of organic matter is over 1% or where the percentage of sulphates is over 0.3%. Stabilizing fine-grained subgrade or subbase with lime is possible. In-situ mixing of soil and stabiliser is typically used for subgrade stabilisation, and 3–6% lime by weight of dry soil is typically required. As a type of lime, quicklime chemically combines with water to produce heat, which can be used for soil stabilization [32]. Since soil moisture is used in the hydration of quicklime, drying the soil is necessary, and the resulting heat can further evaporate soil moisture. Clay particles react with hydrated lime. Mixing causes the calcium ions in the hydrated lime to replace the water and other ions on the surface of the clay particles [33]. Soil becomes granular and friable, facilitating better mixing and compaction. Soil shrink-swell potential and the Plasticity Index both drop significantly. Soil alkalinity rises above 10.5 when lime and water are applied in adequate amounts, leading to the disintegration of clay particles. Calcium from the lime reacts with the freed silica and alumina to generate calcium-silicate-hydrates (CSH) and calcium-aluminate-hydrates (CAH) (CAH) [34]. These cementitious materials help make the ground more robust. Soil undergoes a change from its granular state to that of a hard, generally impermeable material with a high bearing capacity. When it comes to soil stabilisation, quicklime is far and away the best option. However, it is in powder form and reacts violently when exposed to water [35]. As a result, it violates OHS standards. Quicklime dust will be released throughout the application process and will inevitably annoy the neighbours [36].

Drawbacks of Lime Stabilization

There are likely two negative chemical responses in lime-treated soil. The first involves the carbonation of lime, while the second involves a reaction between the soil's sulphate salt and air. When free lime reacts with carbon dioxide in the air, a process known as carbonation takes place [37-39]. However, there are genuine downsides to using calcium carbonate as a cementing ingredient. For starters, its poor bonding means it breaks readily, symbolising where the treated soil is weak. Second, calcium carbonate is a soluble salt and may become powdery after prolonged exposure to air. And since calcium ions are used up during carbonation, the pozzolanic reaction suffers as a result. Soil distress and heaving can occur when calcium-based additions, like lime used in soil stabilisation, come into contact with soluble sulphate salt. Sulfate originates from naturally occurring minerals in the soil, process water, or aquifers. The soil has become more compressible and has less shear strength, among other negative effects. Ettringite and/or thaumasite, both of which contribute to soil instability, are formed when soil calcium and aluminium react with soluble sulphate and water [40-43].

Proposed Method to Stabilise Soils

Soil stabilisation with the use of powdered Industrial Waste Glass is known as "Glass Powder Stabilization." Different types of soil require different analyses, and these are validated by

conducting tests to determine whether or not they are suitable for use with glass powder and, if so, how [44].

Study Area

Orikkai residential building in Kanchipuram District, Tamil Nadu and Valsaravakkam Lake in Porur, Chennai District, Tamil Nadu make up the project's research area. (As seen on Google Maps, the location of the research).

Literature Review

Powdered glass's stabilising impact on clay soil was evaluated by Olutowobi and Ogundosu [5]. The collected glass fragments were crushed into a powder and then mixed with the clay soil at different percentages (18.29.35.10%, 15%), along with the same percentage of cement (base). As a result, the specific gravity and moisture content. The ASSHTO soil classification was determined via studies for particle size distribution and Atterbergs limits. The soil samples were classified as belonging to Group A-6, which has soils with "fair to poor" drainage and subgrade material use, according to the results. Because of this, it was necessary to fortify the ground. The soil was then subjected to a battery of tests, including compaction, California bearing ratio (CBR), and direct shear, both with and without the addition of the powdered glass. Maximum dry density values improved with the addition of powdered glass, and this trend continued until the glass powder content reached 5%, after which it began to drop at 109 and 15%. At 5% glass powder concentration and 5mm penetration, the highest CBR values for the Unsoaked and soaked treated samples were 14.90% and 112.915, respectively. At the glass powder content, the highest values of cohesiveness (17.0) and angle of internal friction (15.0) were recorded [45-49].

According to Fauzi and Djauhari [1], before the construction of the road structure, clayey soil was employed as sod or barrier material to raise the roadway level. Some clays are expansive soil, which can lead to pavement failures and higher than necessary annual road maintenance costs [50-54]. These problems can be traced back to poor techniques used in the original and subsequent pavement designs. In order to reduce pavement failures, it is crucial to advocate for the use of waste plastic and glass to enhance the subgrade soil. High-density polyethylene (HDPE) plastic and crushed glass were tested for their potential as engineering additives for subgrade improvement in this study. Some clayey soil samples were collected from different locations in Kuantan, and tests on their normal compaction, California Bearing Ratio (CBR), and Triaxial strength were undertaken. The CBR of clayey soil samples was generated after four days of soaking at optimal water content. The additive content on stabilised soil ranged from 4% to 8% to 12% of the total dry weight of the soil sample. Integrated Electron Microscopy and Energy- Dispersive X-Ray Spectroscopy were used to study the element (SEM-EDS). The results of the tests demonstrated that the addition of waste HDPE and Glass improved the engineering characteristics and CBR of the stabilised clayey samples. Enhancing the sub-grade strength of soil that will be used in road construction is a top priority if we want to build a better, smoother road [55-59]. Many agencies are working toward this end, and some of them are actively searching for discrete fibres that will affect soil properties like California bearing ratio (CBR) and shear strength. Due to the paucity of research in this area, we will be using glass powder as the discrete fibre in our experiments. We may easily alter the strength of the soil subgrade by incorporating Itot, a novel but useful discrete fibre, into the mix. This can be verified by doing tests to measure CBR values and Atterberg's limits, both of which should increase when using Itot as a reinforcement material [60-68].

According to Ashraf et al. [3], in order to stabilise the black cotton soil, the wastewater bottles are applied to the soils at varying compositions. Compressive strength, liquid limit, and plastic limit tests were the extent of the battery of evaluations. Water will not be absorbed by the conventional proctor tests or by the plastic trash in the soil. The bearing ratio of soil is typically lowered by the

addition of waste water bottles. This research was undertaken by Canakchi et al. [4] to determine if the incorporation of waste soda lime glass powder into clayey soil led to any noticeable changes (WSLGP). Crushed and sieved using a #200 (75um) mesh screen, waste soda lime glasses were added to clay at concentrations of 3.6%, 9.2%, and 12.2% by dry weight of the clay, respectively. After curing, the samples were tested for strength and uniformity [69]. The results of the tests showed that the strength and consistency/properties of clay were drastically altered by the addition of WSLGP [70].

The stabilising effects of three different compounds, including rice husk ash, powdered glass, and cement, on the characteristics of lateritic soil are compared in Kanmodi [2]. Color, moisture content, specific gravity, particle size distribution, and Atterbergs limits were some of the initial studies performed on the lateritic soil to get a sense of its fundamental characteristics [71-74]. Two and a half percent, five percent, seven and a half percent, and ten percent of each stabilising element were combined with the lateritic soil. Between 12.5% and 15% of the total soil mass. The impact of the components on the lateritic soil was next evaluated by conducting compaction and California bearing ratio (CBR) tests on the sample mixtures. The percentage of oxides in the samples was also calculated using chemical analysis. Maximum dry densities of 2.32 g/cm3 (at 25% cement addition), 2.28 g/cm3 (at 5% p powdered glass (PG) addition), and 218 g/cm3 (at 5% rice husk ash (RHA) addition) were obtained in a compaction test, with corresponding optimum moisture contents (OMC) of 10.60%, 14.30%, and 12.41%. CBR studies demonstrated that CBR values increased in all cases as materials were added with those of the cement and powdered glass, yielding the highest values and demonstrating near resemblance under unsoaked conditions. The cement had a lot of oxides, according to the chemistry test. CaO (53.60%), SiO2 (68.45%), and SiO2 (89.84%) were the main components of powdered glass and rice husk ash, respectively [75].

According to Aishwaryalakshmi and Visweshwaran [6], there are many methods for stabilising soil, including cement stabilisation, chemical stabilisation, etc. Lime, cement, and fly powder are just a few examples of materials that can be used to alter soil qualities, along with reinforcement techniques. Stabilization of the soil is one of the standard and most preferable techniques to improve the qualities of the sort, which presents a real issue for civil engineers who must build the substructure over inferior soil like clay. Series of Unconfined Compression (UCC) tests and California Bearing Ratio (CBR) tests are performed on stabilised soil to find the best fibre reinforcement based on the shear soil strengths of the stabilised soil with various fibre combinations. Reinforcing materials can be either natural (coconut cour fibre and Rice husk powder) or manufactured (nylon fibre and glass fibre). A comparison of the results is made, and conclusions are taken about the viability and efficacy of the best fibre reinforcement in increasing soil strength. While several studies have been conducted to stabilise clay using natural or synthetic fibres, the present work combines the two to achieve the best results [76-79]. The optimal ratio of fibres for soil stabilisation is discovered here. Lime is added to waste plastic bottles to stabilise the black cotton soil, as proposed by Manjusha [6]. The soil was tested and compared to standard soil reports. In order to get the desired concentration, the wastewater bottle and lime should be added at the optimal percentage [80-83].

Methodology

Waste plastic, cement, lime, and glass powder are just few of the materials that can be used for soil stabilization Soil amendments including rubber crumbs and fibres. In our experiment, we use varying concentrations of glass powder to stabilise the soil.

Improvement of Soil Stability: The term "soil stabilisation" refers to the method used to increase the soil's stability by enhancing its engineering features. When the available building soil is unfit for the intended purpose, soil stabilisation is a necessity. Compaction, dewatering, and the addition of

materials are just a few of the methods available for stabilising soil. Three different concentrations of glass powder are added to the soil and well mixed to determine the optimal concentration [84-87].

Soil is a collection of organic and inorganic materials, as well as gases, liquids, and creatures that work together to sustain life. The pedosphere, which consists of the Earth's soil, serves as a growing medium for plants, a source of water, a filter for dirty water, and a moderator of the planet's climate. It provides a home for species, and those organisms, in turn, change the soil [88]. The soil acts as a boundary between the underlying lithosphere and the overlying hydrosphere, atmosphere, and biosphere. Polish is a word widely used to describe the ground, which literally means "ground stone" in Polish. Minerals and organic matter form the soil's solid phase, or "matrix," while air and water are contained in the soil's permeable "atmosphere" (the soil solution). Soils are typically viewed as a three-phase system consisting of solids, liquids, and gases [89]. Climate, relief (elevation, orientation, and terrain slope), organisms, and the parent materials (initial minerals) all interact through time to form soil. Erosion and weathering are two of the many physical, chemical, and biological processes that contribute to its ongoing development. Ecologists study soil as if it were an ecosystem due of its complexity and interconnectedness [90-92].

Types of Soil

There are typically five types of soil used by gardeners and farmers. All five consist of sand, silt, and clay, the three main components of soil and the result of weathering rock [93]. The particles in sandy soil are the biggest of any soil type. There are large gaps between the particles, making the texture dry and grainy. Water doesn't stay put on it. Rapid percolation of water makes it impossible for roots, especially those of young plants, to penetrate. Because runoff quickly removes the nutrients from sandy soil, plants have no chance of making better use of them. Sandier ground has the advantage of being easier to work with and warming up faster in the spring. Moistening the soil and rolling it into a ball allows one to examine the predominating soil particle, providing insight on the soil type being worked with [94]. The sandy soil, when rolled between your palms, should not form a ball and should instead crumble readily between your fingers [95].

Silty soil is smooth because its particles are much smaller than those in sandy soil. It becomes soapy and slippery when wet. Between your fingers, when you roll it. Your body still feels dirty. Although silty soil is fairly rich, it has poor nutrient retention and hence cannot be used to its full potential for water retention. Silty soil retains water and is hence unheated and poorly drains. Tramping on silty soil can cause it to become compacted, so be careful when working in the garden. The air quality can deteriorate with time.

Clay soil, with its tiniest particles, is the best at retaining moisture. When wet, it feels sticky, but when dry, it's completely smooth. Little air can move through its spaces since its particles are so small and tend to collect together. It drains more slowly, so it retains more of the nutrient’s plants need. Plants benefit from the abundance of nutrients in clay soil. It takes a while for clay soil to warm up in the spring because the water contained inside it is chilly. Unfortunately, after the clay soil dries out, it may become difficult to work with due to its weight. It may become hard and compact, especially during the heat, restricting your ability to spin it. However, clay soil is often damaged if worked when it is too damp. Clay is formed when damp earth becomes sticky, rolls easily, and can be shaped into a ball or sausage.

Peaty soil is rich in organic matter and has a dark brown or black coloration due to its high-water content and the ease with which it can be compacted. Over nine thousand years ago, as glaciers began to rapidly melt, peat soil began to form. Plants were immediately killed by the flooding caused by this rapid melt. Underwater, their decomposition was so sluggish that organic matter gathered in one location. A good growing medium in the summer, peat soit is often quite wet in the

winter and spring but becomes very dry and flammable in the summer (I kid you not- peat is the precursor of coal). The best thing about peat soil, though, is that it can store water for use during the dry months and shield plant roots from injury during the wetter times of year. Although cannabis water is acidic, gardeners nevertheless include it into their practises as a means of controlling soil diseases and adjusting soil pH. Wet peat soil cannot be rolled into a ball. When squeezed, water can be pushed out of the spongy material.

Saline Soil: Soil in arid climates typically has a high salt concentration, making it taste salty. Saline soil, as it's commonly called, is harmful to plants and can even halt their growth. prevent seeds from germinating and make watering difficult. High salt concentrations limit water uptake by plants, leading to drought stress, and are the cause of the salinity that accumulates in the rhizome sphere. Finding out if your soil is too salty is a simple process. Your plants aren't developing as well as they should, and they have tip burn, especially on their younger leaves. You may also notice a white laver costing the soil's surface.

Where And How Clay Soils Form: Any typical non-choil contains clay properties because of a clay material. Montmorillonite is the most clay-rich of the several clay minerals found on Earth. Soil like these forms when blast rocks are decomposed underwater or when instant clay minerals form from weathering in alkaline conditions. It promotes the synthesis of monilorate when combined with adequate amounts of silica and aluminium. The parent rock is only a few centimetres below the formation's vast soil. These soils are transported and deposited in low-lying and flat locations, where the alluvium deposits can be significantly deeper.

Nature of Expansive Soil

These are two distinct types of clay in clays such as

- Elastic rebounds in compressed soil mass are consequent upon the decrease in compressive force.
- Expansion in water-sensitive clays due to ingress of free water

A later type of clay is referred known as clay. When dry, clayey soils are brittle and, when wet, they show very little cohesion and merging strength, but they don't expand. This causes significant differential settlement and a drop in saturation-level ultimate bearing capacity. Therefore, foundation issues are common in clay soils.

Identification And Classification of Expansive Soils

In order to choose an appropriate foundation or methods to improve expansive clays' behaviour, early identification of expansive nature and preliminary inquiry are needed. Standard categorization results, such as particle size distribution and plastic qualities, provide the basis of common identification skills in engineering practise; other properties used to identify the expanding clay include the following:

- The Clay Minerals: Their Mineralogy.
- Size and shape characteristics of crystals.
- Reaction traits in response to heat treatment.
- Clay particle size and morphology.
- Clay particles have a lack of charge and a high level of surface activity.
- Depending on whether the Clay particles are dry or moist, they will expand.

Glass Powder

Glass is an amorphous, non-crystalline substance that has many practical, technological, and decorative applications. It is commonly used in things like window panes, dishes, and even optics. Rapid cooling (quenching) of the molten form is a common method for creating glass, while other glasses, like volcanic glass, are generated spontaneously. Silica (silicon dioxide, or glass) is the major component of sand and the basis for the most common and oldest varieties of made glass (table 1).

Table 1: Chemical Composition of Glass Powder

Material	Percentage
Silicon dioxide	80.6
Boric oxide	13.0
Sodium oxide	4.0
Aluminium oxide	2.3

Applications of Soil Stabilization

The process of soil stabilisation is useful in the following applications.

- Soil permeability is being decreased.
- Boosting the strength of the soil beneath a building's foundation.
- raising the soil's shear strength.
- Strengthening it so that it can withstand wetness and stress for longer.
- Preparing the land for roads and airports by enhancing the native soils.

The specific gravity of a substance is defined as the ratio of its mass to the mass of a given volume of distilled water at the same temperature. Empty specific gravity or Pycnometer bottle weight (W1). Put the sample into the specific gravity bottle (or Pycnometer). Put dirt in the Pycnometer and weigh it (W). Fill the specific gravity bottle with distilled water until it is about 3/4 full (W). Put the contents through a partial vacuum to remove the trapped air. Note the weight after filling the specific gravity bottle with distilled water to the fill line (W). Clean the specific gravity bottle of any traces of soil and rinse it with distilled water (fig.1).

Figure 1: Pycnometer for Specific Gravity [8]

After Berg's Limit Test

Take a representative soil sample of around 120 gms that fits through a 425 micron IS sieve and thoroughly combine it with distilled water in an evaporating dish to create a homogenous paste for the liquid limit test. The paste should be of a consistency that 30–35 drops from the cup are needed to close the typical groove. For even moisture distribution throughout the soil mass, let the paste sit

for a full day. Before taking the exam, properly re-mix the soil. The California Bearing Ratio Test compares the force needed to enter a soil mass with a standard circular piston at a rate of 1.25 mm/min to the force needed to pierce a standard material at the same rate. The soil sample is sieved using a 3/4-inch (19-mm) mesh sieve. If everything makes it through the sieve, then it's all good to go. However, the sieve may be able to keep some of the particles inside. The material that was kept on the #4 sieve must be replaced with the same volume of material that passed the 3/4-inch sieve. After screening, divide the material into three 6.8-kilogram samples (15 lb). The first specimen will receive 10 blows, the second 30 blows, and the third 56 blows. This will result in a range of possible maximum dry densities, expressed as a percentage. Specimens should have an optimal water content, so it's important to mix in plenty of water.

The extension collar is used to secure the mould to the base plate. After that, we'll take a tally of the mass. Finally, filter paper goes on top of the spacer disc inside the mould. There should be three layers of soil in the mould. Specimen 1 requires 10 rammer blows per layer for compaction, as an example. The material's water content must be measured both before and after compaction. The next step is to get rid of the extension collar and level off the top of the mould using a straight edge. The other two samples need to be compacted in the exact same way. Get rid of the base plate and the spacer disc. The combined weight of the mould and the compacted earth will then be determined. The next step is to flip the soil and mould over and use coarse filter paper to glue the bottom plate to the mould.

Soaking

A standard surcharge weight is 4.54 kilogrammes (kg), which must be placed on the base plate. For around four days, immerse the specimen in water (96 hrs.) The percentage of swell can be calculated by comparing the specimen's pre- and post-soaking height measurements. For this, you can utilise a device designed specifically for measuring expansion. Mold can only come from water after being submerged in it for four days. It is also necessary to get rid of the base plate, filter paper, and surcharge weights. The combined soil and mould mass must be determined.

Put the mould where you want to test the load under the compression machine's penetration piston. On top of the mould, the same additional weight (4.54 kg) must be added. The compressing machine must then be set to deliver a steady stress of 0.05 in (1.27 mm) per minute at the rate of penetration. The loading process will begin with the piston penetrating the ground. The device features dual indicators. The first is a dial gauge, while the second is a proving ring. The proving ring will show how much force was used to break through, and the dial gauge will show how deep you broke through. Please refer to the chart below; the proving ring readings for the penetrations listed in column 1 should be entered in column 2. The piston load will be calculated by multiplying the proving readings by the machine constant (col. 3). Once the piston load (column 4) is known, the penetration stress can be calculated (fig.2)

Figure 2: California Bearing Ratio Test Sample [9]

Put some paste in the cup above where the cup sits on the base, spread it into place with as few spatula strokes as possible, and then trim it to a depth of 1cm at the point of maximum thickness.

Use a grooving tool to cut a precise groove along the cam follower's diameter, passing through its centre. Turning the crank at a pace of two revolutions per second, lower the cup until the two halves of the soil cake touch the bottom of the groove along a distance of approximately 12 mm, or from a height of 10+ 0.25 mm. Keep track of how many water droplets it takes to seal the groove for 12 millimetres. Take a sample of soil that is indicative of the whole and roughly the width of a spatula, cutting across the dirt cake at a right angle to the groove. Let it bake for a whole day. Oven-dried at a temperature between 1050 and 1100 degrees Celsius, and the moisture content is expressed as a percentage of the weight after drying. Empty any residual soil from the cup into the evaporating dish, then scrub both the cup and the grooving tool clean. After adding water to the soil in the evaporating dish to make it more fluid, repeat the procedure described above for at least three more trials (minimum of four). The same procedures for counting blows and measuring moisture content should be used in each circumstance. The uniformity of the samples must be such that no less than 15 and no more than 35 drops are needed to completely fill the groove (fig.3).

Figure 3: Casagrande Liquid Limit Sample [10]

Plastic Limit

The soil mass should be malleable enough to be easily moulded with fingers, therefore 20 grammes of soil should be taken from the section of the material passing the 425 microns IS sieve and thoroughly mixed with distilled water in an evaporating dish. If you're working with clay soil, let the whole bulk sit for 24 hours so the moisture can spread out evenly. Roll a ball containing about 8 grammes of this soil mass between your fingers and the glass plate, as illustrated in Fig. 3, applying enough pressure to roll the material into a thread of uniform diameter along its length. A stroke is defined as the full forward and backward motion of the hand, hence the required rolling rate is somewhere between 80 and 90 strokes per minute. Roll the thread until it breaks exactly at 3 millimetres in diameter. The soil must be kneaded into a homogenous mass and rolled again if the thread doesn't break exactly at 3mm. Repeat the procedure of rolling and kneading the thread until it is smooth. Exact 3mm diameter fragmentation under pressure. Put the soil thread crumbs in a sealed container to see how much moisture is in them. Find the plasticity threshold at a minimum of two locations where the soil passes the IS sieve at 425 microns (fig.4).

Figure 4: Plastic Limit Sample [11]

Standard Proctor Compaction Test of Soil

In the Proctor compaction test, the ideal moisture level at which a specific type of soil will become sufficiently dense and achieve its maximum dry density is determined empirically. To calculate a rough estimate of the soil's natural moisture content, divide a total of 4 x 2 200 g samples among four labelled mixing pans. Determine the ideal soil moisture and the range of watering that will be needed. Aim for a range of 2% in moisture content from sample to sample. Sample No. 3 calls for water, so add it, mix it in well with the soil, and then look at it. If the moisture level is not optimal, add water; modify the amount of water to be added to the remaining samples so that they are all at the same level. Sample 3 (16 percent in the example) may be renamed to sample 4 if, after receiving the necessary estimate of water, it appears overly moist. The amount of water applied to the other samples should be lowered accordingly. The 101.6 mm mild requires a collar, base plate, and Lucite liner to be assembled. The assembly should be placed on the base for compacting. Compact the sample mixture in the mould in five even layers to a total depth of about 127 mm. Use 25 hammer blows, falling freely from a height of 457mm, to compact each layer.

If you want to use the rammer effectively, you need to keep the weight from bouncing off the handle at the top of the stroke. The layer being compressed should receive blows from all directions. After the soil sample has been compressed, the collar may be removed from the mould and a straight edge can be used to level off the top of the sample. Take out the compressed specimen and the liner from the mould, then lift out the base plate from the mould. Measure the weight of the specimen down to the nearest gramme. Remove around 100 grammes of soil from the sample's core, then slice the sample in half vertically to determine its moisture content. Weigh the sample, seal it in a tarred aluminium can, and dry it at 110 degrees Celsius until the weight stays the same. To calculate the moisture content, you must first find the difference between the wet and dry weights and make note of the weight of the moisture. Each of the four samples (two specimens below optimum moisture) will require a second round of compacting and moisture content analyses (fig,5).

Figure 5: Standard Proctor Compaction Test Apparatus [12]

Unconfined Compressive Strength Test

Inspecting the loading frame is the first step. Learn how to operate the hand crank and interpret the strain and load indicators. Learn how to convert the deformation dial gauge's units and the proving ring's calibration constant. The strain rate per minute at which we will be exchanging samples is fifteen percent. Find the strain at 1% by measuring the length of your soil sample. Determine the number of divisions per 1 strain based on the units of the vertical deformation dial gauge. Get some cranking practise in at his specified rate of revolutions per minute. It's crucial that the soil sample isn't sheared at a rate higher than this. 3. Use callipers to determine the soil sample's starting height and diameter. The sample is not likely to be a perfect cylinder. As a result, you'll need to measure the height and width of the soil sample in multiple spots to get an accurate average. To achieve accurate readings, many members of the lab team should take the measurements; if you have any

doubts about how to use the callipers, you should take on the role of laboratory instructor. Get the total (wet) unit weight of the soil sample you took. Load the soil sample into the proving ring, set the dials to zero, and close the loading frame. In this experiment, you will keep track of the amount of force used at various levels of strain. Take measurements at 0, 1, 2, 3, 4, 5, 6, 8, 10, 12, 14, 16, 18, and 20 percent strain. The strain values at which the vertical deformation dial is read should be recorded ahead of time. Using the sample's measured HO as a starting point, the target percentage (fig.6).

Figure 6: Unconfined Compression Test Sample [13]

Results And Discussion

The results of tests conducted on both unstabilized and stabilised soil samples are presented here, along with a comparison of their respective values (figures 7 through 13). (Tables 2 to 13).

Table 2: Specific Gravity Observation 1

S.No	Description	Trial 1	Trial 2	Trial 3
1	Wt. of Dry soil(g)	200	200	200
2	Wt. of Empty Pycnometer(W1)(g)	634	634	634
3	Wt. of Pycnometer + Dry Soil(W2)(g)	834	884	934
4	Wt. of Pycnometer + Soil + Water(W3)(g)	1573	1602	1644
5	Wt. of Pycnometer + Water(W4)(g)	1454	1454	1454
6	Specific Gravity ($G_S = \{ \frac{(w2-w1)}{(w2-w1)-(w3-w4)} \}$	2.47	2.45	2.73

Average Specific Gravity of Soil Sample 1 = 2.56g/cm^3

Table 3: Specific Gravity Observation 2

S.No	Description	Trial 1	Trial 2	Trial 3
1	Wt. of Dry soil(g)	200	200	200
2	Wt. of Empty Pycnometer(W1) (g)	634	634	634
3	Wt. of Pycnometer + Dry Soil(W2) (g)	1140	1120	1139
4	Wt. of Pycnometer + Soil + Water(W3) (g)	1800	1770	1790
5	Wt. of Pyconometer + Water(W4) (g)	1454	1454	1454
6	Specific Gravity ($Gs = \{ \frac{(w2-w1)}{(w2-w1)-(w3-w4)} \}$	2.81	2.47	2.54

Average Specific Gravity of Soil Sample 2 = 2.60g/cm^3

Table 4. Specific Gravity Observation 3

S.No	Description	Trial 1	Trial 2	Trial 3
1	Wt. of Glass Powder(g)	200	200	200
2	Wt. of Empty Pycnometer(W1)(g)	634	634	634
3	Wt. of Pycnometer + Glass Powder(W2)(g)	1534	1535	1534
4	Wt. of Pycnometer + Glass Powder + Water(W3)(g)	2054	2053	2055
5	Wt. of Pycnometer + Water(W4)(g)	1500	1500	1500
6	Specific Gravity ($G_S = \{ \frac{(w2-w1)}{(w2-w1)-(w3-w4)} \}$	2.60	2.58	2.59

Average Specific Gravity of Glass Powder = 2.59g/*cm*

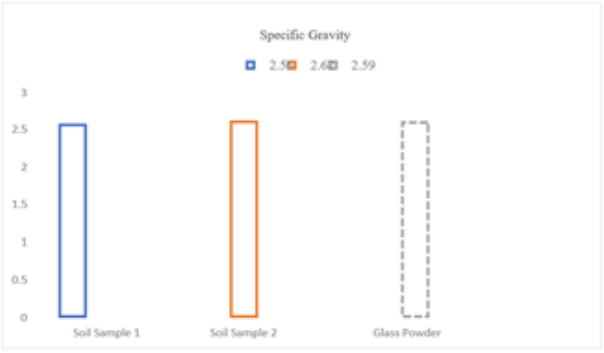

Figure 7: Comparative Study of Specific Gravity

Atterberg Limits: Soil Sample 1

Liquid Limit = 30.7% Plastic Limit = 19.7% Plasticity Index = 11.0% **Soil Sample 2**

Liquid Limit = 34.30% Plastic Limit = 30.158% Plasticity Index = 4.142%

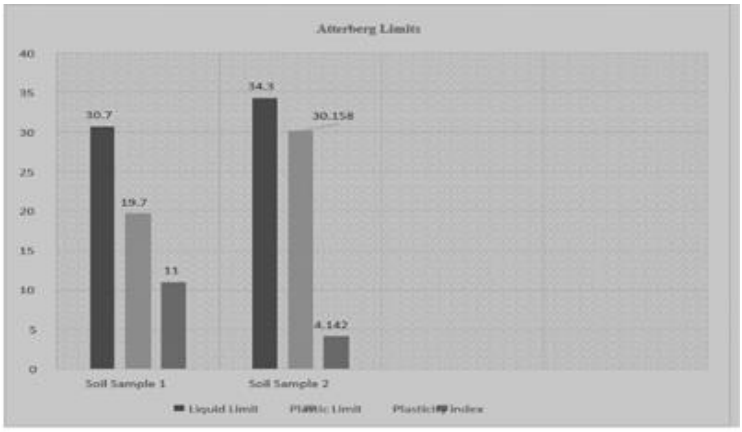

Figure 8: Comparative Study of Atterberg Limits

Table 5: Standard Proctor Compaction Observation 2

S.No	Description	0%	8%	10%	12%
1	Empty mould wt., Kg(W1)	2.000	2.000	2.000	2.000
2	Mould wt., + Sample ,Kg(W2)	3.85	4.01	4.03	3.96
3	Sample wt., Kg(W2 -W1),W3	1.85	2.01	2.03	1.96
4	Mould dia, cm	10.0	10.0	10.0	10.0
5	Mould length, cm	12.7	12.7	12.7	12.7

6	Mould volume ,cm^3(W4)	997.80	997.80	997.80	997.80
7	$W3$Wet density, kg/cm^3( ), $W5$ $W4$	1.85	2.014	2.03	1.964
8	Wet wt , gram(W6)	200	200	200	200
9	Dry wt , gram(W7)	184.5	182.5	179.5	180.95
10	OMC(W6-W7)/(W7,(W8)	8.4	9.58	11.42	10.52
11	MDD(100*W5)/(100+W8)	1.706	1.849	1.8219	1.777

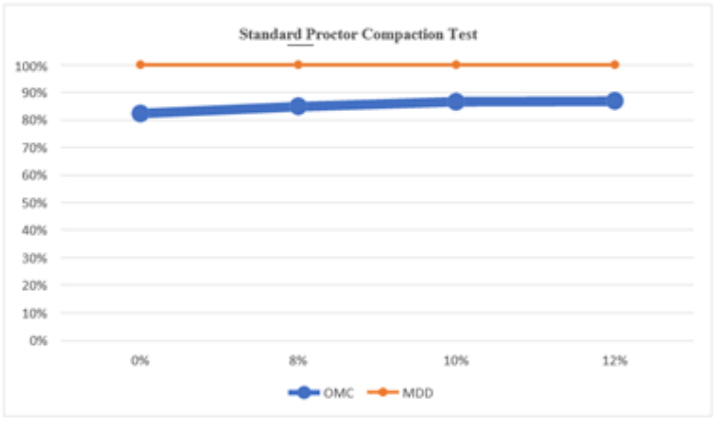

Figure 9: Comparative Study of Standard Proctor Compaction

Table 6: Standard Proctor Compaction Observation 1

S.No	Description	0%	8%	10%	12%
1	Empty mould wt., Kg(W1)	2.000	2.000	2.000	2.000
2	Mould wt., + Sample ,Kg(W2)	3.987	4.033	4.089	3.942
3	Sample wt., Kg(W2 -W1),W3	1.987	2.033	2.089	1.942
4	Mould dia, cm	10.0	10.0	10.0	10.0
5	Mould length, cm	12.7	12.7	12.7	12.7
6	Mould volume ,cm^3(W4)	997.80	997.80	997.80	997.80
7	$W3$ Wet density , kg/cm^3, $W5$, $W4$	1.991	2.037	2.094	1.946
8	Wet wt , gram(W6)	200	200	200	200
9	Dry wt , gram(W7)	184.2	181.25	178.4	179.38
10	OMC(W6-W7)/(W7),(W8)	8.58	10.35	12.11	11.49
11	MDD(100*W5)/(100+W8)	1.834	1.845	1.867	1.745

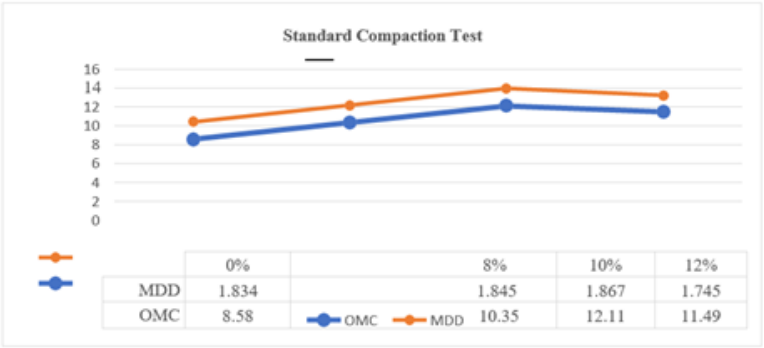

Figure 10: Comparative Study of Standard Proctor Compaction

Table 7: Unconfined Compressive Strength Observation 1

S. No.	Strain Dial, 0.02 MM	Axial Strain (%)	Final area, M^2	Load Dial (0.01 MM)	Axial Load, (T)	Ucc Value, (T/M^2)
1.	0.5	0.59	0.1049	0.14	0.11	1.04
2.	1	1.10	0.1059	0.30	0.39	1.3
3.	1.5	1.76	0.1067	0.71	0.59	5.5
4.	2	2.41	0.1074	1.34	0.80	7.4
5.	2.5	2.97	0.1080	1.50	0.99	9.16
6.	3	3.38	0.1085	2.30	1.07	9.86
7.	3.5	4.00	0.1090	2.79	1.14	10.45
8.	4	4.98	0.1100	3.12	1.00	9.09
9.	4.5	5.15	0.1104	3.71	0.94	5.51
10.	5	5.94	0.1113	4.00	0.89	7.9
11.	5.5	6.21	0.1120	4.97	0.76	6.78
12.	6	7.35	0.1122	6.89	0.69	6.14

Calculation

UCC = Load/Area

= 1.14/1.1090

= 10.45

Table 8: Unconfined Compressive Strength Observation 2

S. No.	Strain Dial, 0.02 MM	Axial Strain (%)	Final area, M^2	Load Dial (0.01 MM)	Axial Load, (T)	Ucc Value, (T/M^2)
1.	0.5	0.63	0.1057	0.17	0.15	1.4
2.	1	1.25	0.1063	0.34	0.42	3.9
3.	1.5	1.88	0.1070	0.76	0.69	6.44
4.	2	2.50	0.1076	1.37	0.81	7.5
5.	2.5	3.13	0.1083	1.54	1.02	9.4
6.	3	3.75	0.1089	2.39	1.18	10.8
7.	3.5	4.38	0.1096	2.84	1.27	11.5
8.	4	5.00	0.1103	3.28	1.43	12.96
9.	4.5	5.63	0.1109	3.79	1.22	11.00
10.	5	6.25	0.1116	4.28	1.05	9.4
11.	5.5	6.88	0.1122	5.23	0.98	8.73
12.	6	7.50	0.1129	7.03	0.87	7.7

Calculation:

UCC = Load/Area

= 1.43/0.1103

= 12.96

Table 9: Comparative Study of Unconfined Compression Test

S.No.	Description	UCC
1.	Soil	10.45
2.	Soil + 8.% Glass Powder	11.67
3.	Soil + 10.% Glass Powder	12.96
4.	Soil + 12.% Glass Powder	10.74

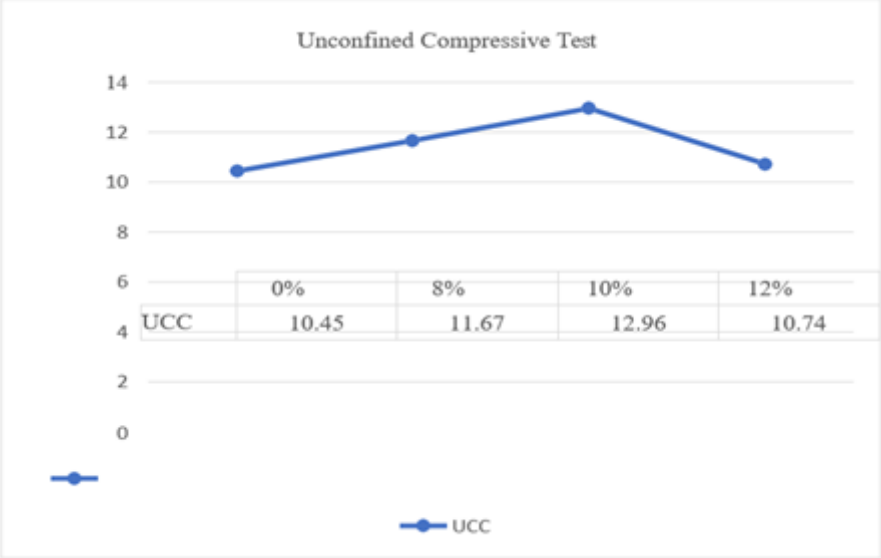

Figure 11: Unconfined Compression Test Comparative Study

Table 10: California Bearing Ration Observation 1

S.No	UNSOAKED (%)			SOAKED (%)		
	Deflection	**Load**	**CBR %**	**Deflection**	**Load**	**CBR%**
1.	0.5	49.38	-	0.5	27.75	-
2.	1	54.15	-	1	35.25	-
3.	1.5	61.75	-	1.5	38.48	-
4.	2	69.25	-	2	45.25	-
5.	2.5	78.78	5.75	2.5	47.81	3.49
6.	3	82.14	-	3	49.75	-
7.	4	92.75	-	4	56.51	-
8.	5	101.72	4.95	5	66.78	3.25
9.	6	109.53	-	6	68.25	-
10.	7.5	117.25	-	7.5	72.47	-
11.	10	123.84	-	10	79.35	-
12.	12.5	132.54	-	12.5	84.48	-

Calculation:

For Table 1, the 2.5mm penetration

CBR = (load applied/standard load) x 100

= (79.78/1370) x 100

= 5.75

For 5mm penetration

CBR = (load applied/standard load) x 100

= (101.72/2055) x 100 = 4.95

Table 11: California Bearing Ration Observation 2

S.No	UNSOAKED (%)			SOAKED (%)		
	Deflection	**Load**	**CBR%**	**Deflection**	**Load**	**CBR%**
1.	0.5	49.14	-	0.5	29.47	-
2.	1	61.25	-	1	37.75	-
3.	1.5	69.74	-	1.5	41.24	-
4.	2	76.45	-	2	49.47	-
5.	2.5	81.65	5.96	2.5	56.44	4.12
6.	3	90.15	-	3	61.48	-
7.	4	99.47	-	4	69.14	-
8.	5	115.69	5.63	5	75	3.65
9.	6	121.45	-	6	79.14	-
10.	7.5	134.85	-	7.5	83.47	-
11.	10	141.75	-	10	91.75	-
12.	12.5	152.28	-	12.5	99.52	-

Calculation:

For Table 2, the 2.5mm penetration

CBR = (load applied/standard load) x 100

= (81.65/1370) x 100

= 5.96

For 5mm penetration

CBR = (load applied/standard load) x 100

= (115.69/2055) x 100

= 5.63

Table 12: Comparative study of CBR Test (Unsoaked)

S.NO	Description	Unsoaked	
		2.5 MM	**5 MM**
1.	Soil	5.75	4.95
2.	Soil + 8% Glass Powder	5.81	5.23
3.	Soil + 10% Glass Powder	5.96	5.63
4.	Soil + 12% Glass Powder	5.67	5.45

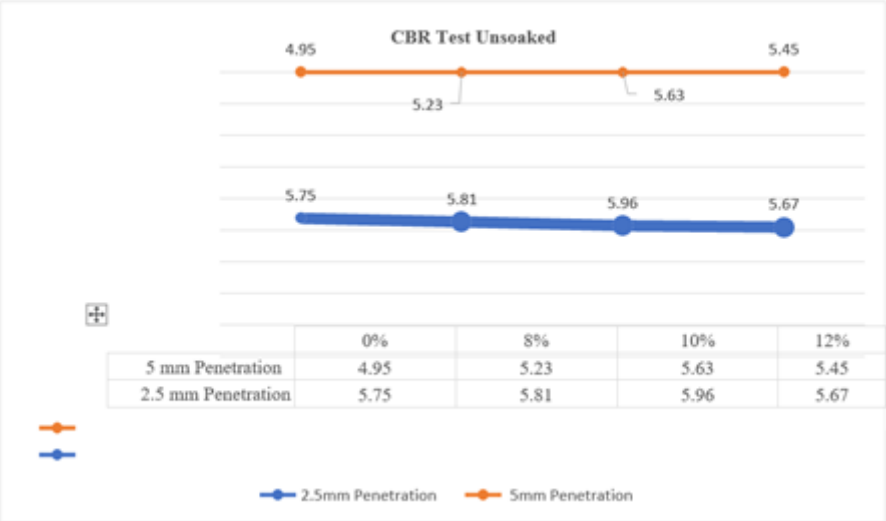

Figure 12: California Bearing Ratio (Unsoaked)

Table 13: Comparative study of CBR Test (Soaked)

S.NO	Description	Soaked	
		2.5 MM	5 MM
1.	Soil	3.49	3.25
2.	Soil + 8% Glass Powder	3.97	3.49
3.	Soil + 10% Glass Powder	4.12	3.65
4.	Soil + 12% Glass Powder	3.98	3.57

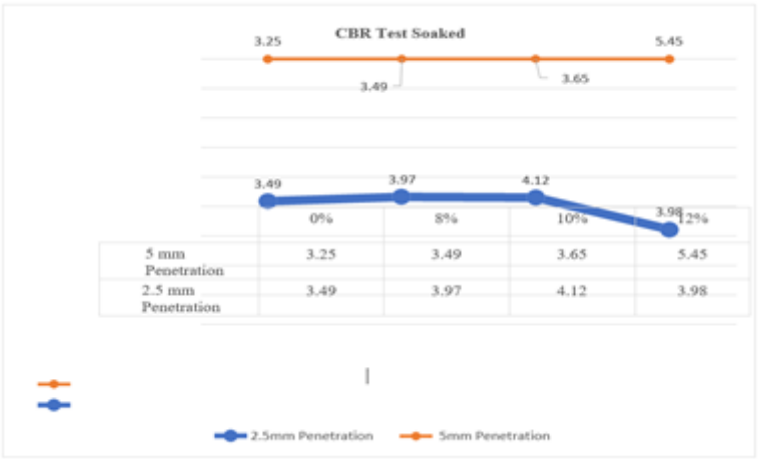

Figure 13: California Bearing Ratio (Soaked)

Conclusion

In this endeavour, glass powder is used to bind the soil together. The samples of both unstabilized and stabilised soil were then put through a battery of tests. With the addition of the glass powder, the results obtained with the clay soil are even more impressive. To optimise the qualities of clay soil, a percentage of glass powder between 8% and 12% by soil mass is recommended. With 10% glass powder content, CBR values reached their highest levels. The greatest CBR values for the stabilised soil were found to be 81.65 percent and 115.69 percent for the Unsoaked and 36.44 percent and 75 percent for the soaked treated samples, respectively, while using 10 percent

powdered glass content. Glass powder as a stabilizing agent has been proven to improve the engineering properties of a clayey soil at a certain concentration; further testing with other soil types is advised.

References

1. A. Fauzi and Z. Djauhari, "Soil engineering properties improvement by utilisation of cut waste plastic and crushed waste glass as additive"," IACSIT International Journal of Engineering and Technology, vol. 8, no. 1, 2016.
2. A. R. J. Kanmodi, "Comparative assessment of rice husk ash, powdered glass and cement as lateritic soil stabilisers"- Article no.16 The Civil Engineering Journal 3," The Civil Engineering Journal, no. 16, pp. 3–2016, 2016.
3. A. Ashraf, A. Sunil, J. Dhanya, M. J. Meera Varghese, and M. Veena, Soil stabilisation using raw plastic bottles"- Indian Geotechnical Conference. Kochi, 2015.
4. H. Canakchi, A. Al Kaki, and F. Celik, "Stabilisation of clay with waste soda lime glass powder"," Journal of Procedia Engineering, pp. 161–600, 2016.
5. J. Olutowobi and A. Ogundosu, "Clay soil stabilisation using powdered glasses," Journal of Engineering Science and Technology, vol. 9, no. 5, 2014.
6. T. Manjusha, "Utilisation of waste bottle plastic strips and lime as a soil stabiliser in construction of flextime pavements"," International Research Journal of Engineering, vol. 4, 2017.
7. V. Aishwaryalakshmi and M. Visweshwaran, "Unconfined compressive Strength behaviour of soil stabilised by various fibre combinations comparative study"," International Journal of Civil Engineering and Technology, vol. 8, pp. 1117–1123, 2017.
8. "Pycnometer bottle, Usage:Chemical Laboratory," indiamart.com. [Online]. Available: https://www.indiamart.com/proddetail/pycnometer-bottle-12981466648.html. [Accessed: 28-Jun-2023].
9. G. Mishra, "California bearing ratio test on subgrade soil -procedure and values," The Constructor, 07-Sep-2010. [Online]. Available: https://theconstructor.org/geotechnical/california-bearing-ratio-test/2578/. [Accessed: 28-Jun-2023].
10. "Liquid limit device," SAP Holdings, 26-Mar-2019. [Online]. Available: https://www.sapholdings.lk/product/liquid-limit-device/. [Accessed: 28-Jun-2023].
11. "Hot Sale Liquid Limit / Plastic Limit Test Accessory Set / Plastic Limit Test Set Apparatus For Soil - Buy Plastic Limit Set Price,Plastic Limit Apparatus,Plastic Limit Test Of Soil Product on Alibaba.com," Alibaba.com. [Online]. Available: https://www.alibaba.com/product-detail/Hot-sale-Liquid-Limit-Plastic-Limit_1600484504699.html. [Accessed: 28-Jun-2023].
12. "Standard Proctor Compaction Test," Civil Engineering Forum, 27-Jun-2017. [Online]. Available: https://www.civilengineeringforum.me/standard-proctor-compaction-test/. [Accessed: 28-Jun-2023].
13. "UCS_failure," ACE Quality Control, 22-Dec-2015. [Online]. Available: https://aceqc.com/profile-2/ucs_failure/. [Accessed: 28-Jun-2023].
14. A.K. Gupta, Y. K. Chauhan, and T Maity, "Experimental investigations and comparison of various MPPT techniques for photovoltaic system," Sādhanā, Vol. 43, no. 8, pp.1-15, 2018.

15. A.K. Gupta, “Sun Irradiance Trappers for Solar PV Module to Operate on Maximum Power: An Experimental Study,” Turkish Journal of Computer and Mathematics Education, Vol. 12, no.5, pp.1112-1121, 2021.
16. A.K. Gupta, Y.K Chauhan, and T Maity and R Nanda, “Study of Solar PV Panel Under Partial Vacuum Conditions: A Step Towards Performance Improvement,” IETE Journal of Research, pp.1-8, 2020.
17. A.K. Gupta, Y.K Chauhan, and T Maity, “A new gamma scaling maximum power point tracking method for solar photovoltaic panel Feeding energy storage system,” IETE Journal of Research, vol.67, no.1, pp.1-21, 2018.
18. A. K. Gupta et al., "Effect of Various Incremental Conductance MPPT Methods on the Charging of Battery Load Feed by Solar Panel," in IEEE Access, vol. 9, pp. 90977-90988, 2021.
19. Satyanaga, H. Rahardjo, and Q. Zhai, “Estimation of unimodal water characteristic curve for gap-graded soil,” Soils and Foundations, vol. 57, no. 5, pp. 789–801, 2017.
20. M. I. Abdou, H. A. Shaban, M. I. El Gohary, “Changes in serum zinc, copper and ceruloplasmin levels of whole body gamma irradiated rats”. Tenth Radiation Physics & Protection Conference, Cairo, Egypt; 27–30 November 2010. pp 17–26.
21. H. A. Shaban, A. A. Shaltout, M. Abdou, E. A. Al Ashker, and M. Elgohary, “Determination of Cu, Zn, and Se in microvolumes of liquid biological samples,” J. Appl. Spectrosc., vol. 77, no. 6, pp. 771-777, 2011.
22. A. A. Shaltout, N. Y. Mostafa, M. S. Abdel-Aal, and H. A. Shaban, “Electron number density and temperature measurements in laser produced brass plasma,” EPJ Appl. Phys., vol. 5, no. 1, pp. 11003–11010, 2010.
23. H. A. Shaban and A. Seeber, “Monitoring global chromatin dynamics in response to DNA damage,” Mutation Research - Fundamental and Molecular Mechanisms of Mutagenesis, vol. 821, no. May–December 2020, p. 111707, 2020.
24. R. Barth and H. A. Shaban, “Spatially coherent diffusion of human RNA Pol II depends on transcriptional state rather than chromatin motion,” Nucleus, vol. 13, no. 1, pp. 194–202, Dec. 2022.
25. R. Barth, G. Fourel, and H. A. Shaban, “Dynamics as a cause for the nanoscale organization of the genome,” Nucleus, vol. 11, no. 1, pp. 83–98, Jan. 2020.
26. H. A. Shaban, R. Barth, and K. Bystricky, “Navigating the crowd: visualizing coordination between genome dynamics, structure, and transcription,” Genome Biology, vol. 21, no. 1, pp. 1-18, 2020.
27. S. R. Vadyala, S. N. Betgeri, J. C. Matthews, and E. Matthews, “A review of physics-based machine learning in civil engineering.” Results in Engineering, vol. 13, p. 100316, 2022.
28. S. R. Vadyala, S. N. Betgeri, and N. P. Betgeri, “Physics-informed neural network method for solving one-dimensional advection equation using PyTorch.” Array, vol. 13, p. 100110, 2022.
29. S. R. Vadyala and E. A. Sherer, “Natural Language Processing Accurately Categorizes Indications, Findings and Pathology Reports From Multicenter Colonoscopy (Preprint).” 2021.
30. S. R. Vadyala, S. N. Betgeri, E. A. Sherer, and A. Amritphale, “Prediction of the number of COVID-19 confirmed cases based on K-means-LSTM.” Array, vol. 11, p. 100085, 2021.
31. O. Fabela, S. Patil, S. Chintamani and B. H. Dennis, "Estimation of effective thermal

conductivity of porous Media utilizing inverse heat transfer analysis on cylindrical configuration," in ASME 2017 International Mechanical Engineering Congress and Exposition, 2017.

32. S. Patil, S. Chintamani, B. Dennis and R. Kumar, "Real time prediction of internal temperature of heat generating bodies using neural network," Thermal Science and Engineering Progress, vol. 23, 2021.
33. S. Patil, S. Chintamani, J. Grisham, R. Kumar and B. H. Dennis, "Inverse Determination of Temperature Distribution in Partially Cooled Heat Generating Cylinder," in ASME 2015 International Mechanical Engineering Congress and Exposition, 2015.
34. Hashem Shatnawi, "Computational Fluid Flow Model for the Development of an Arterial Bypass Graft", CFD Lett., vol. 14, no. 10, pp. 99-111, Oct. 2022.
35. H. A. Shaban and A. Seeber, "Monitoring the spatio-temporal organization and dynamics of the genome," Nucleic Acids Res., vol. 48, no. 7, pp. 3423-3434, Mar. 2020.
36. H. A. Shaban, C. A. Valades-Cruz, J. Savatier, and S. Brasselet, "Polarized super-resolution structural imaging inside amyloid fibrils using Thioflavine T," Sci. Rep., vol. 7, no. 1, pp. 1-10, 2017.
37. R. Barth, K. Bystricky, and H. A. Shaban, "Coupling chromatin structure and dynamics by live super-resolution imaging," Sci. Adv., vol. 6, no. 27, pp. eaaz2196, 2020.
38. H. A. Shaban, R. Barth, L. Recoules, and K. Bystricky, "Hi-D: nanoscale mapping of nuclear dynamics in single living cells," Genome Biol., vol. 21, no. 1, p. 95, 2020.
39. E. Miron et al., "Chromatin arranges in chains of mesoscale domains with nanoscale functional topography independent of cohesin," Sci. Adv., vol. 6, no. 39, pp. eaba8811, 2020.
40. H. A. Shaban, R. Barth, and K. Bystricky, "Formation of correlated chromatin domains at nanoscale dynamic resolution during transcription," Nucleic Acids Res., vol. 46, no. 13, p. e77-e77, Apr. 2018.
41. C. A. Valades Cruz et al., "Quantitative nanoscale imaging of orientational order in biological filaments by polarized superresolution microscopy," Proc. Natl. Acad. Sci., vol. 113, no. 7, pp. E820–E828, 2016.
42. Haq, M. A., Ahmed, A., Khan, I., Gyani, J., Mohamed, A., Attia, E.-A., Mangan, P., & Pandi, D. (2022). Analysis of environmental factors using AI and ML methods. Scientific Reports, 12(1), 13267.
43. Haq, M. A., Ghosh, A., Rahaman, G., & Baral, P. (2019). Artificial neural network-based modeling of snow properties using field data and hyperspectral imagery. Natural Resource Modeling, 32(4).
44. Haq, M. A., & Baral, P. (2019). Study of permafrost distribution in Sikkim Himalayas using Sentinel-2 satellite images and logistic regression modelling. Geomorphology, 333, 123–136.
45. Haq, M. A., Alshehri, M., Rahaman, G., Ghosh, A., Baral, P., & Shekhar, C. (2021). Snow and glacial feature identification using Hyperion dataset and machine learning algorithms. Arabian Journal of Geosciences, 14(15).
46. Mangan, P., Pandi, D., Haq, M. A., Sinha, A., Nagarajan, R., Dasani, T., Keshta, I., & Alshehri, M. (2022). Analytic Hierarchy Process Based Land Suitability for Organic Farming in the Arid Region. Sustainability, 14(4542), 1–16.

47. Rokicki, T.; Koszela, G.; Ochnio L.; Perkowska A.; Bórawski, P.; Bełdycka-Bórawska A.; Gradziuk B.; Gradziuk P.; Siedlecka A.; Szeberényi A.; Dzikuć M. Changes in the production of energy from renewable sources in the countries of Central and Eastern Europe. Frontiers in Energy Research 2022, 10, 993547.

48. Rokicki, T.; Jadczak, R.; Kucharski, A.; Bórawski, P.; Bełdycka-Bórawska, A.; Szeberényi, A.; Perkowska, A. Changes in Energy Consumption and Energy Intensity in EU Countries as a Result of the COVID-19 Pandemic by Sector and Area Economy. Energies 2022, 15(17), 6243.

49. Szeberényi, A.; Lukács, R.; Papp-Váry, Á. Examining Environmental Awareness of University Students. Engineering for Rural Development 2022, 21, pp. 604-611. https://doi.org/10.22616/ERDev.2022.21.TF198

50. Szeberényi, A.; Papp-Váry, Á. Research of Microregion-Related Renewable Energy Tenders for Local Governments. Engineering for Rural Development 2021, 20, pp. 1272-1279.

51. Szeberényi, A. Examining the Main Areas of Environmental Awareness, Sustainability and Clean Energy. In: Daniel Guce; Hayri Uygun; Rashmi Gujrati (ed.), Sustainable Development Goals 2021. Conference: Southampton, United Kingdom, 01.06.2021-18.06.2021., Tradepreneur Global Academic Platform, pp. 258-274.

52. Szeberényi, A. Járás szintű reprezentatív vizsgálat a helyi önkormányzatok megújuló energiával és a környezetvédelemmel kapcsolatos beruházásainak tekintetében. Journal of Central European Green Innovation 2020, 8(1-2), pp. 3-24.

53. Aryal, A., Stricklin, I., Behzadirad, M., Branch, D. W., Siddiqui, A., & Busani, T. (2022). High-Quality Dry Etching of LiNbO3 Assisted by Proton Substitution through H2-Plasma Surface Treatment. Nanomaterials, 12(16), 2836.

54. Paldi, Robynne L., Arjun Aryal, Mahmoud Behzadirad, Tito Busani, Aleem Siddiqui, and Haiyan Wang. "Nanocomposite-seeded Single-Domain Growth of Lithium Niobate Thin Films for Photonic Applications." In 2021 Conference on Lasers and Electro-Optics (CLEO), pp. 1-2. IEEE, 2021.

55. Shifat, A. Z., Stricklin, I., Chityala, R. K., Aryal, A., Esteves, G., Siddiqui, A., & Busani, T. (2023). Vertical Etching of Scandium Aluminum Nitride Thin Films Using TMAH Solution. Nanomaterials, 13(2), 274.

56. Ravinder M and Kulkarni V (2023), Intrusion detection in smart meters data using machine learning algorithms: A research report. Front. Energy Res. 11:1147431.

57. R. M and V. Kulkarni, "Energy-Efficient Algorithm for Cluster Formation and Cluster Head Selection for WSN," 2022 IEEE Bombay Section Signature Conference (IBSSC), Mumbai, India, 2022, pp. 1-6.

58. M. Ravinder and V. Kulkarni, "A Review on Cyber Security and Anomaly Detection Perspectives of Smart Grid," 2023 5th International Conference on Smart Systems and Inventive Technology (ICSSIT), Tirunelveli, India, 2023, pp. 692-697.

59. Szeberényi, A.; Varga-Nagy, A. Az Ökoturizmus jövője – Összehasonlító elemzés a gyöngyösi diákok körében környezettudatossági aspektusból. Studia Mundi – Economica 2017, 4(5), pp. 73-82.

60. Szeberényi, A.; Rokicki, T.; Papp-Váry, Á. Examining the Relationship between Renewable Energy and Environmental Awareness. Energies 2022, 15(19), 7082.

61. Satyanaga & H. Rahardjo, "Unsaturated shear strength of soil with bimodal soil-water

characteristic curve," Geotechnique, Vol. 69, No. 9, pp. 828-832, 2019.

62. Satyanaga, H. Rahardjo & C.J. Hua, "Numerical simulation of capillary barrier system under rainfall infiltration," ISSMGE International Journal of Geoengineering Case Histories, Vol 5, No 1, pp. 43-54, 2019.
63. Kaur, L., & Shah, S. (2022). Production of bacterial cellulose by Acetobacter tropicalis isolated from decaying apple waste. Asian Journal of Chemistry, 34(2), 453–458.
64. Kaur, L., & Shah, S. (2022). Screening and characterization of cellulose-producing bacterial strains from decaying fruit waste. International Journal of Food and Nutritional Science, 11, 8–14.
65. Verma,S & Kaur,L. . (2018). Identification Of Waste Utilizing Bacteria From Fruit Waste. Global Journal for Research Analysis Volume-7(6, June).
66. Kaur, L., & Singh, N., Effect of mustard oil and process variables extrusion behavior of rice grits (2000). Journal Of Food Science And Technology. Mysore, 37, 656–660.
67. Thapar, Lakhvinder. (2017). Bulk And Nano-Zinc Oxide Particles Affecting Physio-Morphological Properties Of Pisum Sativum. International Journal Of Research In Engineering And Applied Sciences (IJREAS).
68. Mathew, Sneha & Thapar, Lakhvinder. (2019). Estimation of Protein Intake on the Basis of Urinary Urea Nitrogen in Patients with Non-Alcoholic Fatty Liver. International Journal for Research in Applied Science and Engineering Technology. 7. 2321-9653.
69. Thapar, Lakhvinder. (2017). Fermentation Potential Of Prebiotic Juice Obtained From Natural Sources. International Journal Of Advanced Research. 5. 1779-1785.
70. Mittal, Srishty & Thapar, Lakhvinder. (2019). Vitamin D Levels Between The Tuberculosis Infected And Non – Infected Subjects In 16-25 Years Of Age.
71. J. J. Patil, Y. H. Patil, A. Ghosh, "Comprehensive and analytical review on optical fiber refractive index sensor", 2020 4th International Conference on Trends in Electronics and Informatics (ICOEI) (48184), IEEE, P. 169-175, June. 15, 2020.
72. H. Bohra, A. Ghosh, "Design and analysis of microstrip low pass and band stop filters", International Journal of Recent Technology and Engineering (IJRTE), Vol. 8, Issue 3, P. 6944-6951, Sept. 2019.
73. Y. H. Patil, A. Ghosh, "Optical fiber humidity sensors: a review", 2020 4th International Conference on Trends in Electronics and Informatics (ICOEI) (48184), IEEE, P. 207-213, June. 15, 2020.
74. J. J. Patil, Y. H. Patil, A. Ghosh, "Fiber Optics Refractive Index Sensor based on Intensity Modulation", 2020 4th International Conference on Electronics, Communication and Aerospace Technology (ICECA), IEEE, P. 623-628, May. 2020.
75. H. Bohra, A. Ghosh, A. Bhaskar, A. Sharma, "A miniaturized notched band microstrip wideband filter with hybrid defected ground structure technique", 2020 Third International Conference on Smart Systems and Inventive Technology (ICSSIT), IEEE, P. 745-750, Aug. 2020.
76. Y. H. Patil, J. J. Patil, A. Gaikwad, A. Ghosh, "Development of Optical Fiber Test Bench for Intensity-Modulated Optical Fiber Sensors", 2020 4th International Conference on Trends in Electronics and Informatics (ICOEI) (48184), IEEE, P. 176-180, June. 2020.

77. H. Bohra, A. Ghosh, "A Review on Different Optimization Techniques for Selecting Optimal Parameters in Microstrip Bandpass Filter Design", International Journal of Advanced Science and Technology, Vo. 28, Issue 14, P. 379-394, Nov. 2019.
78. J. Terdale, A. Ghosh, "An intensity-modulated optical fiber sensor with agarose coating for measurement of refractive index", International Journal of System Assurance Engineering and Management, Springer India, P. 1-7, Nov. 2022.
79. J. J. Patil, A. Ghosh, "Intensity Modulation based U shaped Plastic Optical Fiber Refractive Index Sensor" 2022 6th International Conference on Trends in Electronics and Informatics (ICOEI), IEEE, P. 18-24, Apr. 2022.
80. H. Bohra, A. Ghosh, A. Bhaskar, "Design and Analysis of Spurious Harmonics Suppressed Microstrip Ultrawide Band Filter using Modified Defected Ground Structure Techniques", Wireless Personal Communications, Springer US, Vol. 121, Issue 1, P. 361-380, Nov. 2021.
81. H. Bohra, A. Ghosh, A. Bhaskar, A. Sharma, "A Miniaturized Ultra-Wideband Low-Pass Microstrip Filter Design using Modified Defected Ground Structure Techniques", Invertis University, Vol. 14, Issue 1, P. 25-30, 2021.
82. S. S. Priscila, S.S. Rajest, S. N. Tadiboina, R. Regin and S. András, "Analysis of Machine Learning and Deep Learning Methods for Superstore Sales Prediction," FMDB Transactions on Sustainable Computer Letters., vol. 1, no. 1, pp. 1–11, 2023.
83. A. Ghosh, P. Chakrabarti, P. Siano, "Approach towards realizing the Security Threats for Mobile IPv6 and Solution Thereof", International Journal of Computer Applications, Foundation of Computer Science, Vol. 90, Issue 10, Jan. 2014.
84. A. Ghosh, P. Chakrabarti, D. Bhatnagar, "Performance Evaluation of Optimized Mobile IP Protocol Vis-à-vis Bit Map Indexing Method", International Journal of Computer Applications, Foundation of Computer Science, Vol. 75, Issue: 2, Jan. 2013.
85. H. Patidar, P. Chakrabarti, A. Ghosh, "Parallel Computing Aspects in Improved Edge Cover Based Graph Coloring Algorithm", Indian Journal of Science and Technology, Vol. 10, P. 25, Jul. 2017.
86. Praveen Kumar Sharma, Sushil Sharma, Common fixed point for weakly compatible maps in intuitionistic fuzzy metric spaces using property (S-B)", Journal of Non-linear Analysis Optimization and Theory, Vol 5, No.2 (2014), 105-117.
87. Praveen Kumar Sharma, Sushil Sharma, Common fixed point theorem in intuitionistic fuzzy metric space under strict contractive conditions", Journal of Non-linear Analysis Optimization and Theory Vol 3 No.2 (2012), 161-169.
88. Praveen Kumar Sharma, Common fixed points for weakly compatible maps in intuitionistic fuzzy metric spaces using the property (CLRg)", International Knowledge Press, Asian Journal of Mathematics & Computer Research, Vol 6, No.2 (2015), 138-150.
89. Praveen Kumar Sharma, Shivram Sharma, Common Fixed Point Theorems for Six Self Maps in FM-Spaces Using Common Limit in Range Concerning Two Pairs of Products of Two Different Self-maps", Revista Geintec-Gestao Inovacao E Tecnologias, Vol 11, No. 4 (2021), 5634-5642.
90. Shivam Sharma, Praveen Kumar Sharma,A study of SIQR model with Holling type–II incidence rate", Malaya Journal of Matematik, Vol. 9, No. 1, 305-311.
91. A. I. Zannah, S. Rachakonda, A. M. Abubakar, S. Devkota, and E. C. Nneka, "Control for Hydrogen Recovery in Pressuring Swing Adsorption System Modeling," FMDB Transactions

on Sustainable Energy Sequence, vol. 1, no. 1, pp. 1–10, 2023.

92. Satyanaga & H. Rahardjo, "Role of unsaturated soil properties in the development of slope susceptibility map," Geotechnical Engineering. Vol 175, No 3, pp. 276-288, 2022.
93. Satyanaga & H. Rahardjo, "Stability of unsaturated soil slopes covered with Melastoma Malabathricum in Singapore," Geotechnical Engineering. Vol 7, No 6, pp. 393-403. 2020.
94. Satyanaga, H. Rahardjo, Z.H. Koh & H. Mohamed. "Measurement of a soil-water characteristic curve and unsaturated permeability using the evaporation method and the chilled-mirror method," Journal of Zhejiang University-SCIENCE A. Vol 20, No 5, pp. 368-375, 2019.
95. Satyanaga, N. Bairakhmetov, J.R. Kim & S.-W. Moon. "Role of bimodal water retention curve on the unsaturated shear strength," Applied Sciences. Vol 12, No 3, pp. 1266. 2022